DESIGN OF SEISMIC RESTRAINERS FOR IN-SPAN HINGES

By Panos Trochalakis,[1] Marc O. Eberhard,[2] Member, ASCE, and John F. Stanton,[3] Member, ASCE

ABSTRACT: A reinforced concrete, box-girder bridge will collapse during an earthquake if the relative displacement between adjacent frames at an in-span expansion joint exceeds the available seat width. To identify factors that most affect these relative displacements, 216 nonlinear response-history analyses were conducted for various frame, abutment, and restrainer properties, as well as for four ground motions. The researchers considered only longitudinal motion of straight bridges without skew, and the ground motions were assumed to be coherent. Maximum relative joint displacements were sensitive to the stiffnesses of adjacent frames, the frames' effective periods, and the restrainer properties. The relative displacement between the frames and abutment seats was sensitive to the overall stiffness and weight of the bridge. Based on the results of the parametric study, new design procedures are proposed for designing in-span seismic restrainers and abutment seats. Examples illustrate both procedures. Compared with existing design methods, the proposed methods result in restrainer designs that are more consistent with the results of nonlinear analysis.

INTRODUCTION

Most bridges have movement joints to accommodate thermal expansion and contraction without inducing large forces in the bridge. During an earthquake, the joints pose a hazard. If the relative displacement of adjacent frames or girders exceeds the available seat width, the span will collapse.

In cast-in-place concrete box girders, a joint is usually placed near the natural point of inflection, at about 20% of the span. Since such joints offer no moment resistance, they are usually referred to as in-span hinges. Box girders constructed before 1971 are particularly vulnerable to unseating because their in-span hinges usually have narrow seats, on the order of 150 mm. Fig. 1 shows such a box-girder bridge, in which the girder came close to unseating during the 1994 Northridge earthquake.

Following the collapse of several bridges during the 1971 San Fernando earthquake, many state and local agencies began installing seismic restrainers in existing and new bridges to prevent excessive relative movements of frames. These restrainers usually consist of steel cables or rods. Most retrofit programs (Lwin and Henley 1993) assign a high priority to installing such devices because the cost of restrainer installation is relatively low and because span unseating has catastrophic consequences. Despite this high priority, the methods available for designing seismic restrainers are inadequate (Yang 1994).

The purpose of this paper is to propose a new method for designing restrainers at in-span hinges for straight bridges with little skew. The proposed method is similar to a method adopted by the California Department of Transportation (Caltrans) (*Seismic* 1990), but the new method is more consistent with the results of nonlinear analyses. The paper also presents a method for estimating the maximum relative displacement at the abutment. This displacement places a lower bound on the required abutment seat width.

[1]Struct. Engr., KPFF Consulting Engrs., 1201 3rd Ave., Ste. 900, Seattle, WA 98101.

[2]Assoc. Prof., Dept. of Civ. Engrg., Univ. of Washington, Box 352700, Seattle, WA 98195.

[3]Prof., Dept. of Civ. Engrg., Univ. of Washington, Box 352700, Seattle, WA.

Note. Associate Editor: Nicholas P. Jones. Discussion open until September 1, 1997. To extend the closing date one month, a written request must be filed with the ASCE Manager of Journals. The manuscript for this paper was submitted for review and possible publication on August 25, 1995. This paper is part of the ***Journal of Structural Engineering***, Vol. 123, No. 4, April, 1997. ©ASCE, ISSN 0733-9445/97/0004-0469–0478/$4.00 + $.50 per page. Paper No. 11468.

EXISTING DESIGN METHODS

The two most widely used restrainer design methods are those adopted by the American Association of State Highway and Transportation Officials (AASHTO) (*AASHTO* 1994) and Caltrans (*Seismic* 1990).

AASHTO Method

According to the AASHTO specifications (1994), restrainers are required if the available seat width, measured parallel to the bridge's longitudinal axis, is less than an empirically-determined minimum value, N.

$$N = (200 + 0.0017L + 0.0067H)(1 + 0.000125S^2) \quad (1)$$

where L = length of bridge deck adjacent to joint (mm); H = average height of adjacent columns (mm); and S = skew of support (degrees). All lengths are expressed in mm, and the skew angle is expressed in degrees. The minimum support width is further multiplied by a factor of 1.5 in zones 3 and 4. If the length provided is less than the minimum length, restrainers must be installed. The only guidance that AASHTO provides for proportioning the restrainers is that the restrainer's strength should be greater than or equal to the seismic acceleration coefficient times the weight of the lighter frame adjacent to the hinge (*AASHTO* 1994).

The AASHTO method is attractively simple, but it does not take into account some important factors, such as the stiffnesses and periods of the frames adjacent to the hinge. Also, the method does not provide estimates of the minimum required restrainer stiffness and the maximum relative hinge dis-

FIG. 1. In-Span Hinge on Verge of Collapse (1994 Northridge Earthquake)

placement (MRHD). Without these estimates, the designer cannot have confidence that the selected restrainer is short enough to provide the necessary stiffness yet long enough to prevent yielding.

Caltrans Method

The Caltrans method (*Seismic* 1990) is more complex than the AASHTO method. First, the designer computes the MRHD at which seating loss would occur, D_r. Next, the designer estimates the force-deflection relationship of each of the two adjacent frames, including the resistance provided by the restrainers and abutments. The nominal displacement response for each frame (D_1 and D_2) is determined from the equivalent elastic stiffness at displacement D_r, the frame weight, and a design response spectrum. The predicted MRHD is taken as D_s, the smaller of the two displacements. Design consists of increasing the restrainer stiffness until D_s falls below D_r. The restrainer length is chosen so that the restrainer will not yield before it reaches the elongation D_r.

Saiidi et al. (1992) and Yang (1994) evaluated the Caltrans method. Saiidi et al. (1992) considered a three-frame model with abutments, while Yang (1994) performed a parametric study of a two-frame model without abutments. Both studies concluded that the results of the Caltrans method were inconsistent with the results of nonlinear time history (NLTH) analysis and that, in some cases, the Caltrans method underestimated the MRHD.

STANDARD BRIDGE MODEL

To evaluate the influence on response of varying the bridge properties, it was necessary to develop many analytical models. The prototype for these models consisted of two frames, two abutments, and a single in-span hinge. Each prototype frame was supported by two or more column bents connected by an inextensible superstructure. The corresponding analytical models were variations of the standard bridge model shown in Fig. 2. The properties of the standard model are given in column 2 of Table 1.

Frames

The resistance of each frame was modeled by a horizontal spring with bilinear stiffness, for which the force-displacement

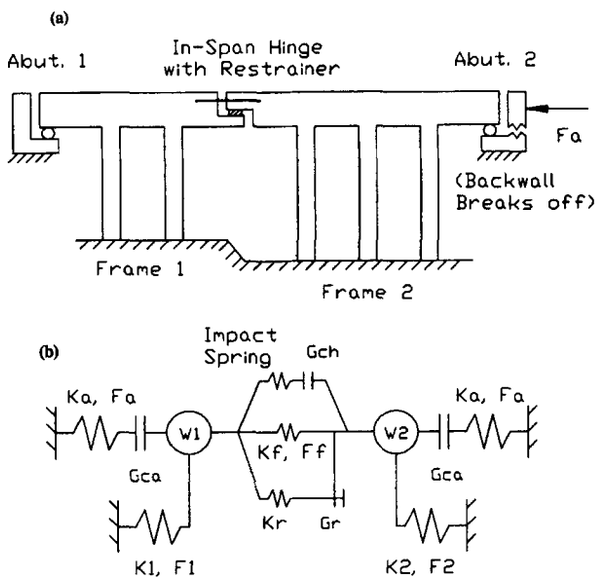

FIG. 2. Models: (a) Prototype; (b) Analytical (Note: Abutment, Frame, and Friction Springs Are Bilinear)

TABLE 1. Element Properties for Analytical Models

Parameter (1)	Values for standard models (2)	Ranges varied in parametric study[a] (3)
(*a*) Frame 1		
Stiffness, K_1[b]	105 kN/mm	50, 100, 200%
Strength, F_1	4.00 MN	80, 100, 125%
Weight, W_1	22.2 MN	50, 100, 200%
(*b*) Frame 2		
Stiffness, K_2[b]	105 kN/mm	5–2000%
Strength, F_2	4.00 MN	37–271%
Weight, W_2	22.2 MN	not varied
(*c*) Abutments		
Stiffness, K_a	700 kN/mm	0, 100, 200%
Strength, F_a	5.56 MN	0, 100, 200%
Compression gap, G_{ca}	25 mm	same as for hinge gap
(*d*) Hinge		
Restrainer stiffness, K_r	175 kN/mm	0, 25, 50, 100, 150, 200, 250%
Restrainer gap, G_r	25 mm	0, 100, 200, 300%
Impact stiffness	17.5 MN/mm	not varied
Compression gap, G_{ch}	25 mm	0, 50, 100, 150%
Friction stiffness, K_f	26.3 kN/mm	0, 100%
Friction force, F_f	0.44 MN	0, 100%

[a]Ranges expressed as percentage of standard values.
[b]Postyield stiffness was equal to 2% of preyield stiffness.

relationship was the sum of the resistances provided by the column bents. The weight of each frame ($W_1 = W_2 = 22.2$ MN) was selected to reflect typical Washington State Department of Transportation bridges and to be compatible with the weights considered by Yang (1994). The number of columns was computed from the assumed weight based on the assumptions that the columns were 1.22 m square, the concrete compressive strength was 34.5 MPa, and the axial stress due to dead load was 10% of the concrete compressive strength. It was further assumed that the reinforcing steel was grade 60 and that the column longitudinal reinforcement ratio was 1%, which led to a column yield strength, M_y, of 3,570 kN·m. The calculated cracked moment of inertia ($I_{cr} = 0.053$ m^4) was approximately equal to 30% of the gross-section moment of inertia. The calculations of both I_{cr} and M_y included the influence of axial load.

The initial stiffness, K, and yield force, F, of the frames were computed as follows:

$$K = (\text{number of columns}) \cdot 7.5EI_{cr}/H^3 \quad (2)$$

$$F = (\text{number of columns}) \cdot 2M_y/H \quad (3)$$

where E = elastic modulus of the concrete; and H = frame column height (7.62 m in the standard model). This initial stiffness corresponds to the average stiffness of a cantilever ($3EI_{cr}/H^3$) and a column fixed at both ends ($12EI_{cr}/H^3$). For the purpose of the nonlinear analysis, the postyield stiffness was taken as 5% of the initial stiffness. In the standard model, frames 1 and 2 had the same properties.

Abutments

The abutment prototype (Fig. 2) consisted of a seat, which is supported on piles, cast monolithically with a backwall. In an actual bridge, the girder would rest on bearings that would offer some resistance, but this resistance was neglected. After the gap (G_{ca}) between the girder and backwall has closed, the abutment resistance increases significantly. At larger displacements, the backwall breaks off (*Seismic* 1990) and the soil properties dictate the subsequent backwall resistance. The

abutment model was a simplification of the prototype. In the model, both the seat's lateral resistance and the backwall's resistance before failure were neglected. The study did not consider the effect of installing restrainers at the abutments.

The backwall was represented by a massless node that was connected on one side to a gap element that simulated the deck joint and on the other, to an elasto-plastic spring that simulated the soil resistance (K_a, F_a). The deck-joint gap element ensured that the soil spring would be loaded in compression only. Properties for the nonlinear springs were derived from the Caltrans guidelines (*Seismic* 1990). The recommended soil stiffness and strength simplify to $19bh^2$ kN/mm and $150bh^2$ kN, where b = width; and h = height of backwall. The resulting stiffness, K_a, and strength, F_a, are listed in Table 1 for b = 11.0 m and h = 1.83 m. Soil-structure interaction was not considered in the study.

Hinge

The prototype hinge detail contained a deck joint, a bearing pad to transfer vertical loads across the hinge, and restrainers (Fig. 2). Similarly, the hinge model included three components. Collision of the two frames when the deck joint closed was modeled with a linear spring that was effective in compression only. The standard hinge compression gap (G_{ch}) was assumed to be 25 mm wide, and the stiffness of the impact spring was assumed as 17.5 MN/mm to be consistent with the work of Yang (1994).

The restrainers were modeled with a linear spring that was effective in tension only (Fig. 2). Typically, restrainers are installed with slack under the anchor nut to avoid restraining thermal movements in the bridge. Consequently, the restrainer stiffness was assumed to become effective only after a 25-mm-wide restrainer gap (G_r) closed. The standard restrainers were assumed to consist of four 38-mm-diameter steel rods, each 5.3 m long. Based on an elastic modulus of 207 GPa, the standard restrainer stiffness, K_r, was computed to be 175 kN/mm.

The third element at the hinge was a "friction" element, whose yield force corresponded to the shear force required to initiate slip in the prototype. The friction element represented a series of 25-mm-thick elastomeric pads with a total vertical load of 2.2 MN and a coefficient of friction of 0.2 (Stanton and Roeder 1982). These pads were assumed to have a shear modulus of 1 MPa and to be proportioned to limit the bearing stress to 3.43 MPa. These assumptions led to a stiffness, K_f, of 26.3 kN/mm and a slip force, F_f, of 440 kN (Table 1).

RESPONSE HISTORY FOR STANDARD MODEL

The standard earthquake input motion was the N·S component of the 1940 El Centro earthquake, multiplied by a factor of 2.0 to give a peak acceleration of $0.70g$. The response of analytical models to this motion was computed with nonlinear time history analysis (Prakash et al. 1993). In the computations, the viscous damping ratio for the first two modes was assumed to be 5%.

Displacement responses for frames of the standard model are plotted in Fig. 3(a), in which displacements to the right (Fig. 2) are defined as positive. The two frames moved in unison (as expected, because the dynamic characteristics of the frames were identical) until frame 1 collided with abutment 1. Frame 1 had a maximum displacement of 147 mm away from abutment 1 approximately 3.0 s into the earthquake. Frame 2 had a maximum displacement of 102 mm away from abutment 2 at approximately 12 s. The amount of opening or closing that the hinge experienced at any time could be determined by calculating the difference between the frame 1 and frame 2 displacements. The largest joint opening, defined as the MRHD, was 14 mm; it occurred 12.4 s into the ground motion.

Both abutments yielded within the first two seconds of the earthquake [Fig. 3(b)]. The final displacement of the abutment 1 backwall slightly exceeded 50 mm, and the abutment 2 backwall final displacement was nearly 90 mm. To determine the likelihood of unseating at the abutment, one might assume that the abutment displacements [Fig. 3(b)] must be added to the frame displacements [Fig. 3(a)] to obtain the maximum relative abutment displacement (MRAD). However, the abutment backwall was modeled as shearing off during the earthquake, and the piles would likely keep the abutment seat near its initial position. Therefore, the MRAD was taken as the maximum displacement of either frame relative to the original abutment location. This definition is slightly unconservative because the abutment seat would likely move relative to the ground during the earthquake. As shown in Fig. 3(a), the MRAD in this case was equal to the maximum positive displacement for frame 1 (147 mm). In other cases, the MRAD corresponded to the maximum negative displacement for frame 2.

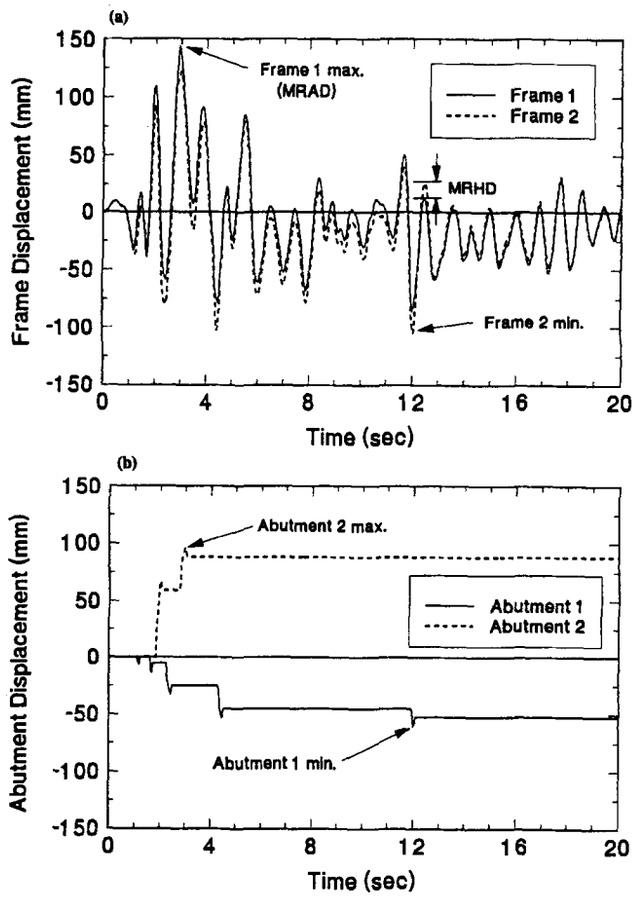

FIG. 3. Displacement Histories for Standard Bridge Model: (a) Frames; (b) Abutment Backwalls

PARAMETRIC STUDY

The influence of each model parameter on the response of the standard bridge model was evaluated by varying the parameters one at a time and performing nonlinear time history analyses. Ranges for the parameter variations are given in column 3 of Table 1. The stiffnesses and strengths were not varied independently; they were varied to correspond to column heights ranging from 3 to 21 m. Trochalakis et al. (1996) provide details of the analyses.

Effect of Frame Stiffnesses, K_1 and K_2

The effects of the frame stiffnesses on the MRHD and MRAD are illustrated in Fig. 4. The results of two types of

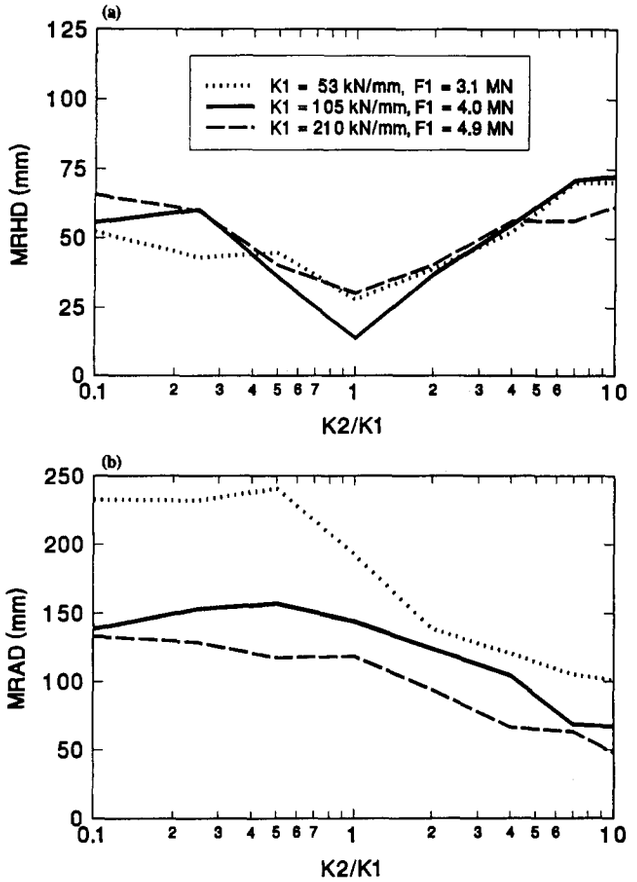

FIG. 4. Effects of Frame Stiffness on: (a) MRHD; (b) MRAD

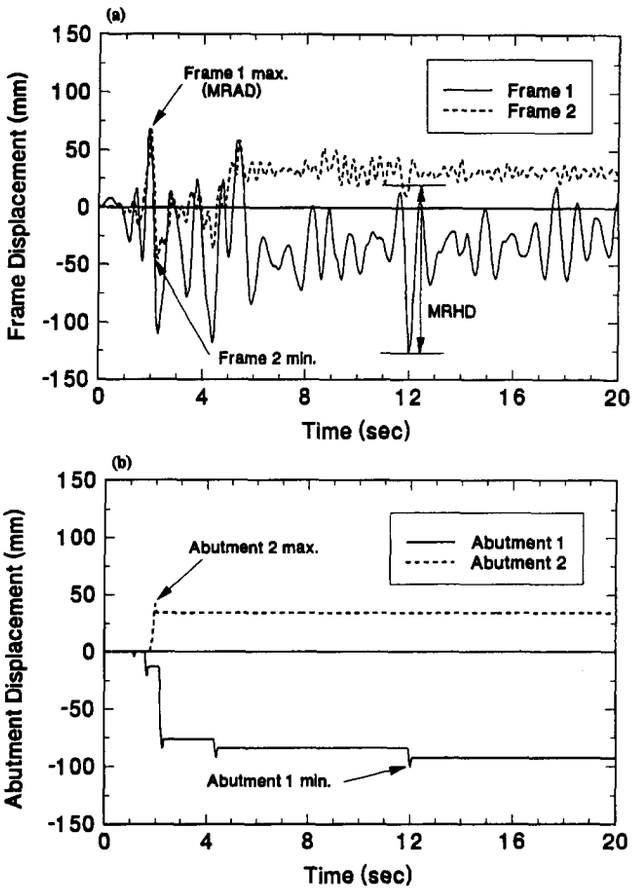

FIG. 5. Displacement Histories for $K_2/K_1 = 7.0$ and $K_r = 0.0$

variation are shown. First, K_1 was kept constant at its standard value (105 kN/mm) and K_2 was varied from $0.1K_1$ to $10K_1$. The yield forces were also adjusted [(3)], because the variation in K_2 implies a variation in the column heights from 3.5 to 16.4 m [(2)]. These results are represented by the solid lines in Fig. 4. Fig. 4(a) shows that the MRHD was smallest when $K_2 = K_1$, and it increased with the ratio of the frame stiffnesses. This trend is explained by the fact that the frames oscillated nearly in phase when their periods were similar. In contrast, the responses of the frames differed greatly when $K_2/K_1 = 7.0$, K_1 had its standard value, and $K_r = 0$, as shown in Fig. 5. Frame 2 had a much shorter period than frame 1, and the two frames oscillated independently. The other two curves in Fig. 4(a) show the effects of changing K_1 and then varying K_2/K_1 from 0.1 to 10. Again, the MRHDs were smallest when the frame periods were nearly equal. This observation is consistent with the results of Yang (1994).

The maximum relative abutment displacement (MRAD) decreased when the ratio K_2/K_1 increased and when K_1 itself increased [Fig. 4(b)]. This trend demonstrates the influence of the total stiffness, $K_1 + K_2$. As expected, the stiff bridges had small displacements and small MRADs.

Effects of Frame 1 Weight

The effects of changing the weight of frame 1 (W_1), while holding W_2 constant are shown in Fig. 6. Again, as in Fig. 4, this effect was investigated for K_2/K_1 ranging from 0.1 to 10. In Fig. 6(a), the solid line is for standard values of W_1 and W_2. For all three curves, the minimum MRHD occurred when $K_2/K_1 = W_2/W_1$. This observation is consistent with the behavior illustrated in Fig. 4. The MRHDs were smallest when the frames had identical periods. Doubling W_1 substantially in-

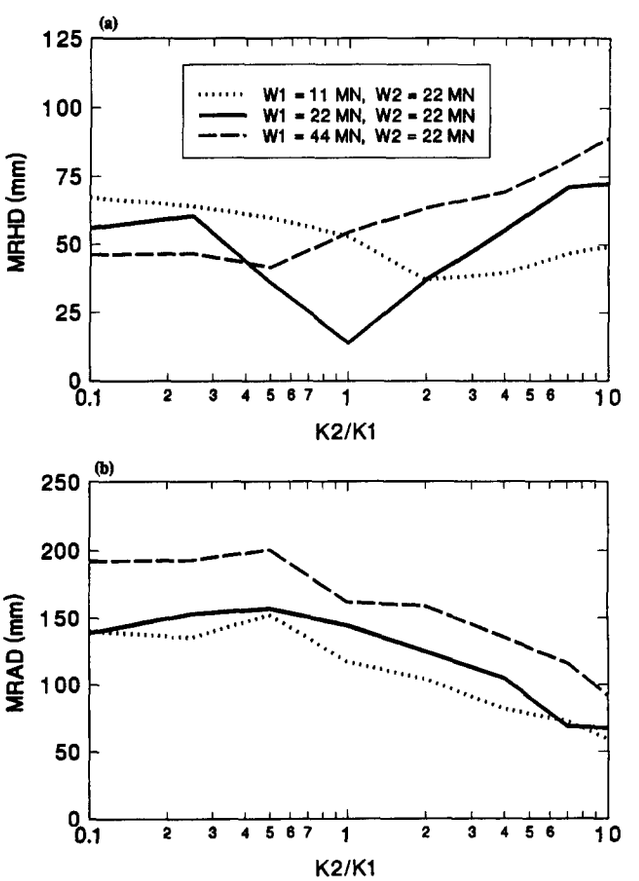

FIG. 6. Effects of Frame Weight on: (a) MRHD; (b) MRAD

creased the MRAD but halving it only slightly decreased the MRAD [Fig. 6(b)].

Effects of Abutment Strength and Stiffness

The stiffnesses (F_a) and strengths (K_a) of the abutments were first doubled and then both were set to 0.0. Fig. 7(a) shows that modifying the abutment properties had little influence on the MRHD. As expected, the MRHD was exactly zero when the abutment resistance was eliminated and the frame stiffnesses were identical.

The MRADs increased significantly when the abutment resistance was eliminated, especially when K_2/K_1 was small [Fig. 7(b)]. In those cases, frame 2 was flexible and it underwent large displacements because there was no abutment to limit its movement.

Effects of Restrainer Stiffness

The influence of the restrainer stiffness is shown in Fig. 8. Fig. 8(a) shows that the restrainers were effective in reducing the MRHD. The restrainers had little effect when K_2/K_1 was close to 1.0 because the frames tended to move in phase regardless of the restrainer properties. The restrainer properties had little effect on the MRAD [Fig. 8(b)].

Effects of Restrainer Gap

Fig. 9 shows the effects of the restrainer gap (G_r). Increasing the restrainer gap increased the MRHD. When the frame stiffnesses differed significantly, the MRHD was approximately equal to the MRHD for $G_r = 0.0$ plus the provided G_r. In other words, the restrainer elongation was nearly independent of the restrainer gap for these cases. The observation that the re-

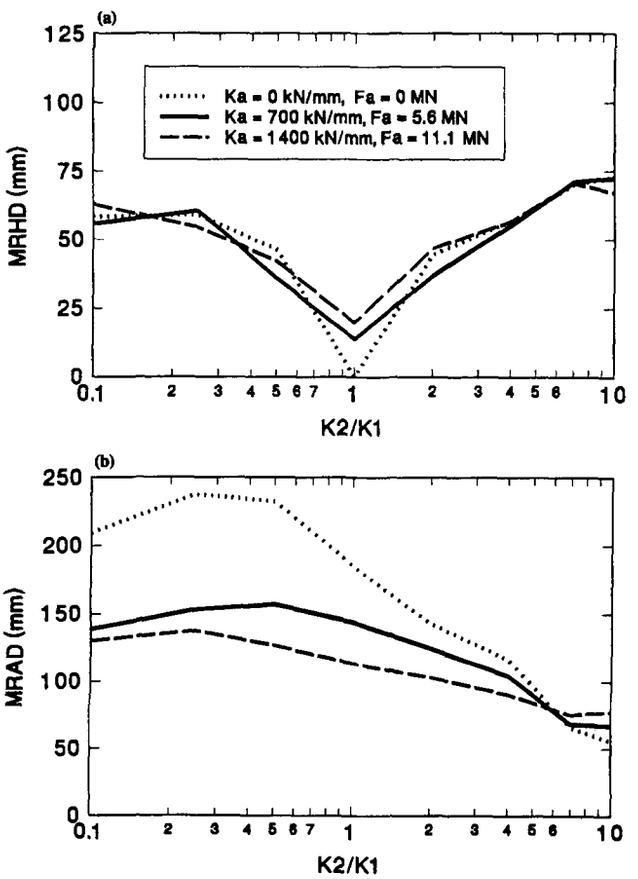

FIG. 7. Effects of Abutment Properties on: (a) MRHD; (b) MRAD

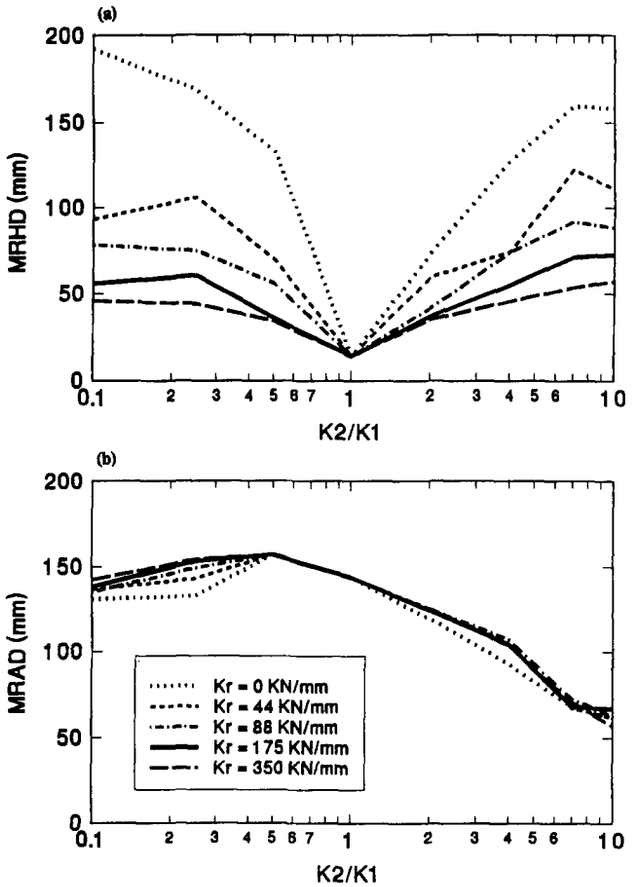

FIG. 8. Effects of Restrainer Stiffness on: (a) MRHD; (b) MRAD

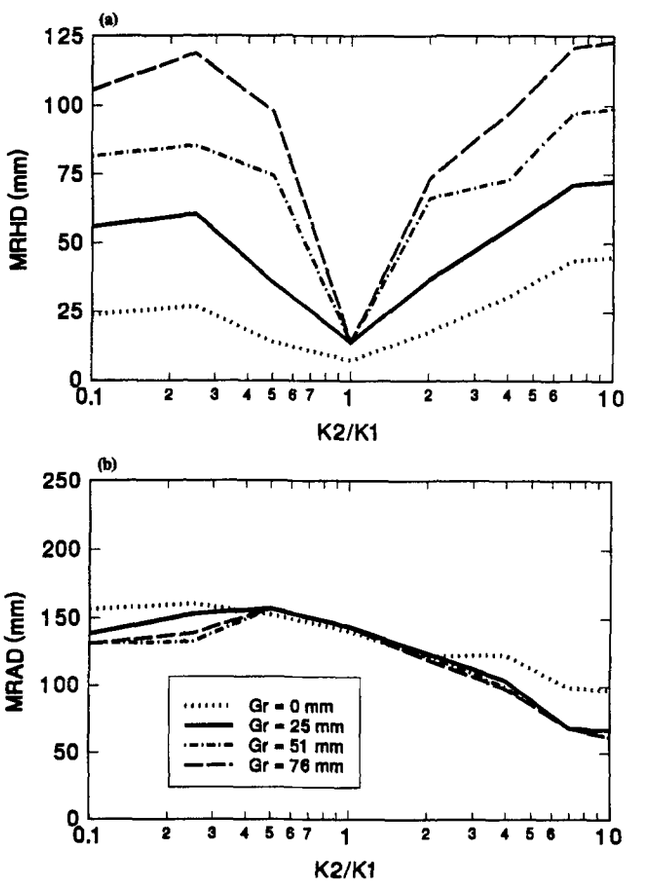

FIG. 9. Effects of Restrainer Gap on: (a) MRHD; (b) MRAD

strainer gap greatly affects the MRHD has a practical consequence. It is common to make the restrainer gap considerably larger than the expected thermal movements. Such excessive restrainer gaps should be avoided because they directly affect the MRHDs. The restrainer gap barely affected the MRAD.

Effects of Other Parameters

The effects of Coulomb friction at the hinge, the size of the compression gaps and thermal expansion of the deck were also considered. None of these parameters significantly affected the MRHD or MRAD (Trochalakis et al. 1996).

PROPOSED RESTRAINER DESIGN METHOD

The Caltrans method (*Seismic* 1990) has some features that are attractive. In particular, the use of the equivalent stiffness of the frames on either side of the hinge accounts for the structural properties of the frames, and the spectral displacement demands (D_1 and D_2) reflect the ground motion. Restrainer design consists of increasing the restrainer stiffness until the MRHD falls below the allowable MRHD. These features are included in the proposed method.

However, Yang (1994) showed that it is unreasonable to assume that the MRHD is equal to D_s, the smaller of D_1 and D_2. Therefore, a new basis for estimating the MRHD was sought. The new procedure reflects the average displacement demand for the two frames, D_{avg}, and the ratio of the two oscillator effective periods, T_L/T_s. The new procedure consists of the following steps:

Step 1

Compute the allowable MRHD

allowable MRHD = seat width

$-$ minimum allowable bearing width $- G_{ch}$

where G_{ch} = hinge compression gap.

Step 2

Construct the force-displacement relationship for the equivalent single degree of freedom (SDOF) system consisting of the structure on one side of the hinge. One frame is moved away from the hinge while the other is held in place. Each abutment contributes to resistance only after the adjacent compression gap closes. In implementing the design method, the frames are assumed to have a linear force-deflection relationship, while the abutments are assumed to have an elasto-plastic force-deflection relationship. An example of such a force-deflection relationship is shown in Fig. 10 for $K_2/K_1 = 7.0$. Fig. 10(a) shows the force-displacement relationship for frame 1 (Table 1) as it moves to the left, and Fig. 10(b) shows the force-displacement relationship for frame 2 as it moves to the right. The changes in slope correspond to points at which the abutment gap closes and the soil behind the abutment yields. The x-axis offset in each restrainer curve corresponds to the restrainer gap.

Step 3

Select a trial displacement (Δ_{trial}) for the SDOF system representing all of the components on one side of the hinge.

Step 4

For Δ_{trial}, calculate the equivalent system stiffness, K_s

$$K_s = (\text{force required to produce } \Delta_{trial})/\Delta_{trial} \quad (4)$$

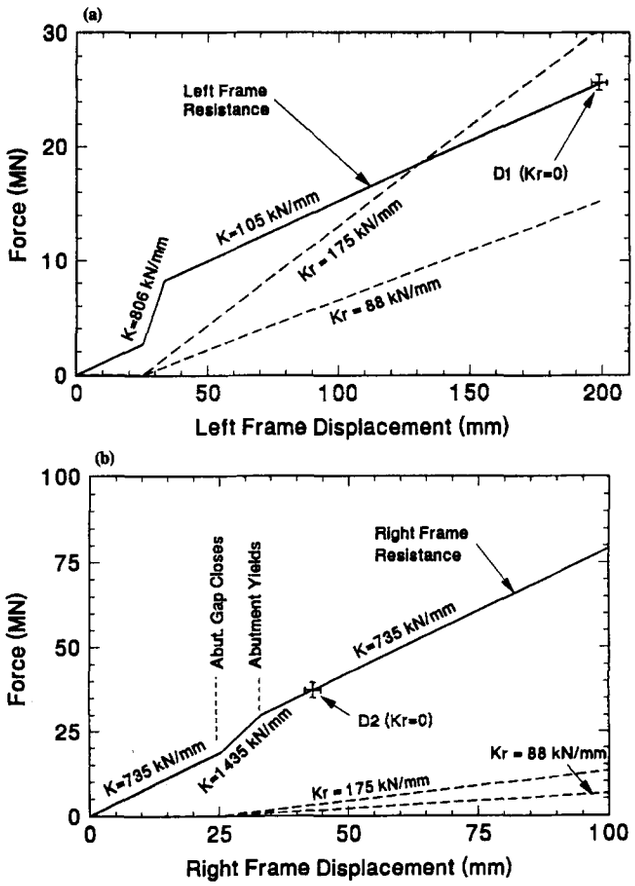

FIG. 10. Force-Deformation Relationships for $K_2/K_1 = 7.0$ and $K_r = 0.0$; (a) Frame 1; (b) Frame 2

Step 5

Calculate the effective restrainer stiffness, $K_{r,eff}$

$$K_{r,eff} = K_r \cdot (\Delta_{trial} - G_r)/\Delta_{trial} \quad \text{if } \Delta_{trial} > G_r \quad (5a)$$

$$K_{r,eff} = 0.0 \quad \text{if } \Delta_{trial} \le G_r \quad (5b)$$

Step 6

Compute the total equivalent stiffness

$$K_t = K_s + K_{r,eff} \quad (6)$$

Step 7

Calculate the equivalent period, T

$$T = 2\pi \sqrt{\frac{W}{K_t \cdot g}} \quad (7)$$

where W = weight of all mobilized frames, and g = acceleration due to gravity.

Step 8

Calculate the equivalent single-degree-of-freedom displacement

$$\Delta_{sdof} = \text{ARS} \cdot W/K_t \quad (8)$$

where ARS = acceleration response spectral ordinate from a smoothed response spectrum [Fig. 11(a)] for the equivalent period, T.

Step 9

Repeat steps 3–8 until $\Delta_{sdof} = \Delta_{trial}$. Define D_1 as the final displacement.

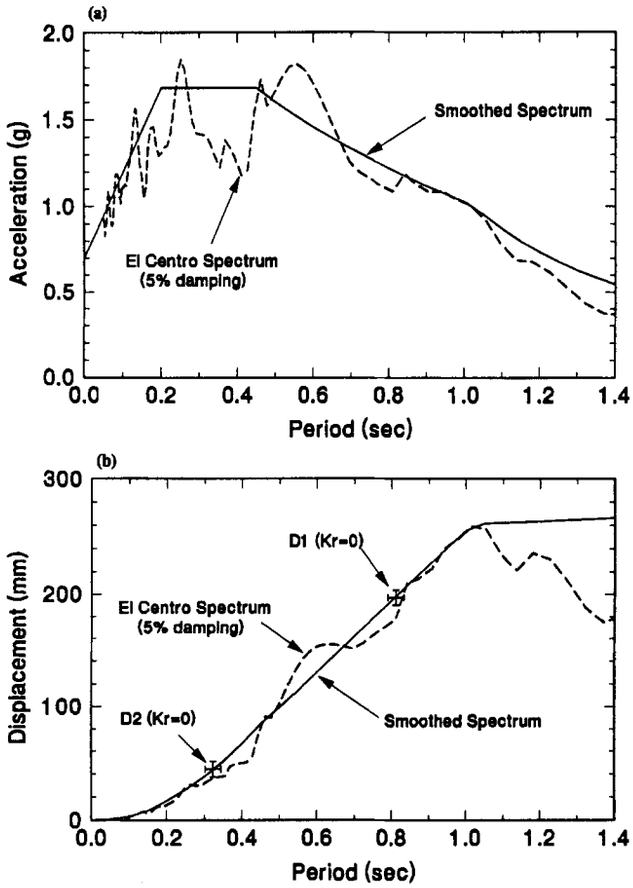

FIG. 11. 1940 El Centro Ground Motion: (a) Acceleration; (b) Displacement Response Spectra

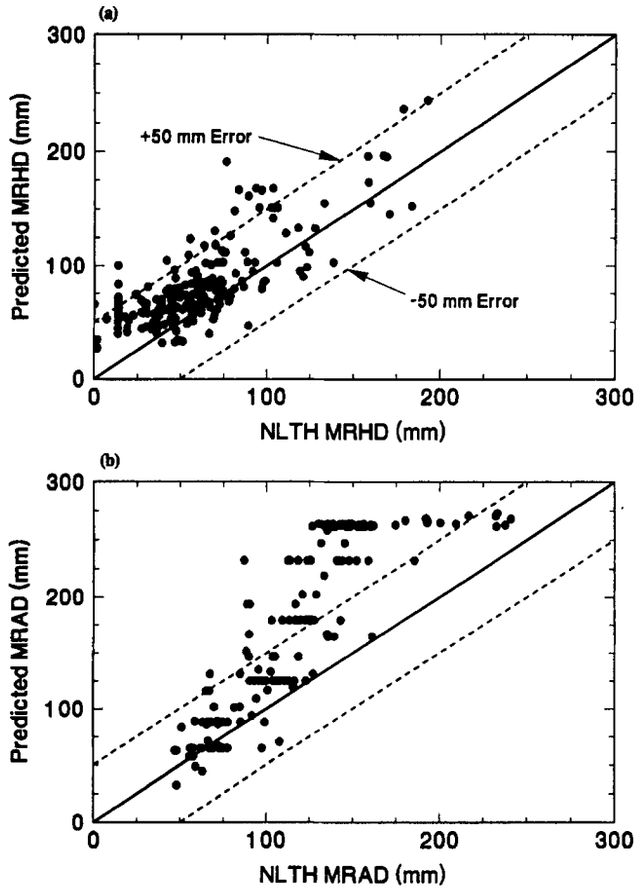

FIG. 12. Comparison of Proposed Methods with NLTH for: (a) MRHD; (b) MRAD

Step 10

Repeat steps 2–9 for the other side of the hinge to obtain D_2.

Step 11

Compute the predicted MRHD

$$\text{MRHD} = \frac{D_{\text{avg}}}{2}\frac{T_L}{T_s} \leq D_1 + D_2 \tag{9}$$

where $D_{\text{avg}} = (D_1 + D_2)/2$; T_L = larger equivalent period; and T_s = smaller period.

Step 12

Modify the restrainer stiffness and repeat steps 2–11 until the predicted MRHD is less than or equal to the allowable MRHD.

Step 13

Select a suitable combination of restrainer length and area to provide the required stiffness and to ensure elastic behavior.

All the database cases were analyzed with the proposed method to compare the results with those of nonlinear time-history (NLTH) analysis. The mean of the absolute differences between the MRHD predicted by the proposed method and NLTH was 25 mm; the largest unconservative error was 42 mm [Fig. 12(a)].

EXAMPLE RESTRAINER DESIGN

The proposed procedure is illustrated for the standard bridge (Table 1 and Fig. 2) and ground motion (Fig. 11) but with $K_2/K_1 = 7.0$. The design problem consists of selecting a restrainer stiffness that will limit the predicted MRHD to less than the allowable MRHD. For the example, the properties listed in Table 1 were supplemented with the assumptions that the seat width was 190 mm and that the minimum allowable bearing width was 75 mm. The computed response histories for the El Centro ground motion, multiplied by 2.0, are shown in Fig. 5 for $K_r = 0.0$.

As described in step 1, the allowable MRHD was calculated as 190 − 75 − 25 = 90 mm. Steps 2–11 were then implemented for the unrestrained case ($K_r = 0.0$), as shown in Table 2 and Figs. 10 and 11. The predicted MRHD of 154 mm (Table 2) agreed well the MRHD of 159 mm computed by NLTH analysis (Fig. 5). Since the predicted MRHD exceeds the allowable MRHD (90 mm), restrainers are required to limit the relative hinge displacements. By repeating steps 3–11 for a restrainer stiffness of 88 kN/mm, the predicted MRHD was reduced to 102 mm. Since this value exceeds 90 mm, the restrainer stiffness was further increased to 175 kN/mm, and the predicted MRHD was reduced to 86 mm, which is acceptable.

To ensure that the restrainers remain elastic, their yield displacement must exceed MRHD − G_r = 61 mm. For rods, with E = 207 GPa and F_y = 830 MPa, the minimum restrainer length is 15.3 m, and the corresponding restrainer area is 12,900 mm^2. Assuming cables with E = 70 GPa and F_y = 1.2 GPa, the restrainer length is reduced to 3.5 m, and the area is 8,800 mm^2.

PROPOSED ABUTMENT SEAT WIDTH CALCULATION METHOD

A new method for estimating the unrestrained maximum relative abutment displacements also was developed. The par-

TABLE 2. MRHD Estimate for Unrestrained Example Bridge

Step number (1)	Left-Hand Side of In-Span Hinge		Right-Hand Side of In-Span Hinge
	First trial (2)	Second trial (3)	First trial (4)
2	see Fig. 10(a)	see Fig. 10(a)	see Fig. 10(b)
3	Δ_{trial} = 127 mm	Δ_{trial} = 196 mm	Δ_{trial} = 43 mm
4	K_s = (127 · 105 + 5,560)/127 = 149 kN/mm	K_s = (196 · 105 + 5,560)/196 = 133 kN/mm	K_s = (43 · 735 + 5,560)/43 = 866 kN/mm
5	$K_{r,eff}$ = 0 · (127 − 25)/127 = 0 kN/mm	$K_{r,eff}$ = 0 · (196 − 25)/196 = 0 kN/mm	$K_{r,eff}$ = 0 · (43 − 25)/43 = 0 kN/mm
6	K_t = 149 + 0 = 149 kN/mm	K_t = 133 + 0 = 133 kN/mm	K_t = 866 + 0 = 866 kN/mm
7	$T = 2\pi\sqrt{\frac{22{,}200}{149 \times 9{,}810}} = 0.774$ s	$T = 2\pi\sqrt{\frac{22{,}200}{133 \times 9{,}810}} = 0.820$ s	$T = 2\pi\sqrt{\frac{22{,}200}{866 \times 9{,}810}} = 0.321$ s
8	ARS = 1.24g [Fig. 11(a)]; Δ_{sdof} = 1.24 · 22,200/149 = 185 mm	ARS = 1.24g [Fig. 11(a)]; Δ_{sdof} = 1.19 · 22,200/133 = 199 mm	ARS = 1.24g [Fig. 11(a)]; Δ_{sdof} = 1.68 · 22,200/866 = 43 mm
9	$\Delta_{trial} \neq \Delta_{sdof}$	$\Delta_{sdof} \cong \Delta_{trial}$; D_1 = 199 mm [Figs. 10(a) and 11(b)]	$\Delta_{sdof} = \Delta_{trial}$; D_2 = 43 mm [Figs. 10(b) and 11(b)]
10	—	see table column 4	—

Note: For step 11 D_{avg} = (199 + 43)/2 = 121 mm; T_L/T_s = 0.820/0.321 = 2.55; MHRD = (121/2) · (2.55) = 154 mm.

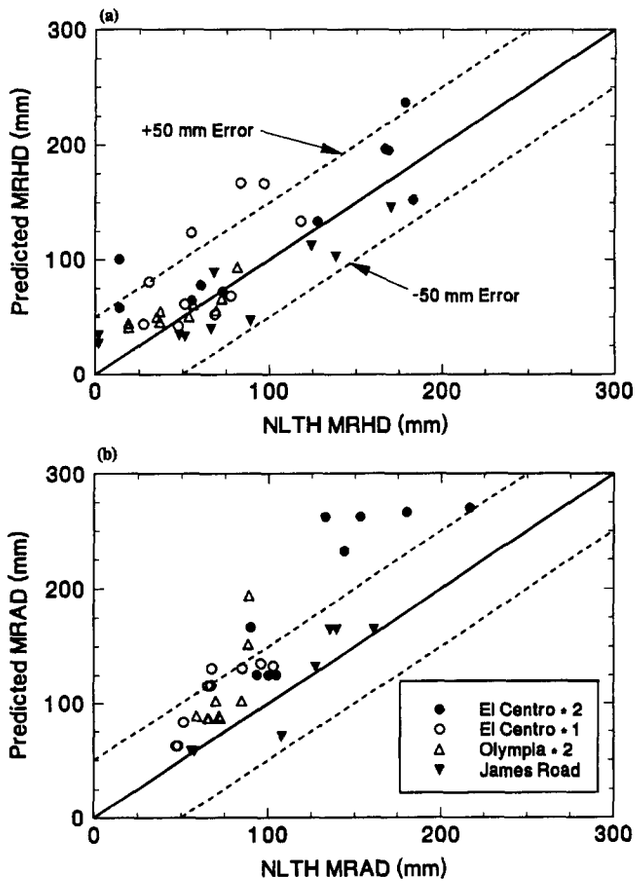

FIG. 13. Effects of Ground-Motion Characteristics on: (a) MRHD; (b) MRAD

ametric study showed that the following variables are important in predicting the MRAD: (1) abutment stiffness and strength; (2) sum of frame stiffnesses; and (3) sum of frame weights. An approach that incorporated all three variables was first examined. The same procedure used to compute the SDOF displacements for each side of the in-span hinge was used to compute the SDOF displacement for the entire bridge moving away from one of the abutments. In this case, the predicted MRAD was equal to the SDOF displacement.

This equivalent stiffness method worked well (Trochalakis et al. 1996), but it required iteration. A noniterative procedure gave results that correlated nearly as well as the iterative procedure with the results of NLTH analysis. In the noniterative procedure, the entire bridge is treated as a single frame, and the abutments and compression gaps are ignored. The simpler procedure reduces the calculation effort and the chance for error. The MRAD can be estimated as follows

- Step 1: Calculate the equivalent SDOF period, T

$$T = 2\pi \cdot \sqrt{\frac{\Sigma W}{\Sigma K \cdot g}} \tag{10}$$

where ΣW = sum of all frame weights; ΣK = sum of all frame stiffnesses; and g = acceleration due to gravity.

- Step 2: Calculate the predicted maximum relative abutment displacement, MRAD

$$\text{MRAD} = \text{ARS} \cdot (\Sigma W/\Sigma K) \tag{11}$$

where ARS = spectral acceleration (in g) corresponding to period T.

- Step 3: Compute the minimum acceptable seat width

$$\text{Minimum acceptable seat width} = G_{ca} + \text{Minimum allowable bearing width} + \text{MRAD} \tag{12}$$

The MRADs predicted by the proposed method for the database are compared with the values computed with NLTH analysis in Fig. 12(b). The scatter was larger than for the MRHD predictions (mean error = 60 mm), but the unconservative error exceeded 25 mm in only two of 216 cases.

EXAMPLE SEAT-WIDTH CALCULATION

This procedure was applied to the standard ground motion and bridge (Fig. 2) but with K_2/K_1 = 7.0. For the example, it was assumed that the minimum allowable bearing width was 75 mm.

- Step 1: ΣW = (2 · 22.2 MN) = 44.4 MN; ΣK = 105 kN/mm + (7 · 105 kN/mm) = 840 kN/mm; and T = 0.46 s.
- Step 2: MRAD = 1.68g · 44,400 kN/(840 kN/mm) = 89 mm; in comparison, the MRAD computed by NLTH analysis was 68 mm [Fig. 5(a)].
- Step 3: Minimum acceptable seat width = 25 mm + 75 mm + 89 mm = 189 mm; if the existing seat were narrower than 189 mm, it would need to be extended.

APPLICATION OF PROPOSED PROCEDURES TO NEW SITUATIONS

The proposed methods for predicting the MRHD and MRAD were developed from the results of the parametric study, in which 85% of the analyses were performed for El Centro ground motion, multiplied by a factor of 2.0. Also, all the structures in the database were two-frame bridges whose

columns had a stiffness coefficient of 7.5 [(2)]. It is necessary to consider whether the method gives acceptable results in other situations.

Effects of Ground Motion Characteristics

The standard model and nine variations on it were subjected to four ground motions: the 1940 El Centro motion multiplied by 2.0, the unmodified 1940 El Centro motion, the 1949 Olympia motion multiplied by 2.0, and the James Road record from the 1979 Imperial Valley earthquake. Soil-structure interaction was neglected. Despite the variations in ground-motion characteristics, Fig. 13(a) shows that the MRHDs were well predicted by the proposed method. For the James Road and Olympia ground motions, the mean MRHD error was 20 mm, and the largest unconservative error was 42 mm. The mean error for the MRAD was 25 mm, and in all but one of 40 analyses, the results were conservative [Fig. 13(b)].

Effects of Column Damage

An additional 12 models were analyzed to investigate the effects of column damage, simulated by assuming that the column bases were pinned. This assumption is recommended by Caltrans for situations in which the column flexural resistance is likely to deteriorate with cyclic loading (*Seismic* 1990). For the standard bridge (H = 7.62 m), the stiffness ($3EI_{cr}/H^3$) and strength (M_y/H) were 44 kN/m and 2.0 MN, respectively. Standard values were assumed for the abutment properties (Table 1), ground motion and viscous damping. Two sets of six analyses were conducted. In each, K_1 remained constant while K_2/K_1 was assigned values of 0.5, 1, 2, 4, 7, and 10. In the first set the restrainer stiffness was 175 kN/mm and in the second, it was zero.

Fig. 14 shows the MRHDs and MRADs predicted by the proposed method plotted against the values obtained from NLTH analysis. The values for corresponding undamaged frames are included for comparison. For the damaged frames, the mean error was 40 mm for both the MRHD and the MRAD.

Effects of Number of Frames

Ten analyses were conducted on three-frame models to observe the effect of increasing the number of frames (Trochalakis et al. 1996). Although the proposed method was developed for two-frame bridges, the method provided acceptable results for three-frame bridges also (Fig. 14). For the three-frame bridges, the MRHD mean error was 35 mm, and the MRAD mean error was 75 mm.

COMPARISON WITH OTHER METHODS

The proposed method [Fig. 12(a)] for estimating the MRHD better approximates NLTH analysis than the Caltrans method [Fig. 15(a); mean error = 53 mm], particularly in cases where adjacent frames have similar masses and stiffnesses. The effort necessary to implement the two methods is similar; all 216 cases were analyzed with a single spreadsheet.

There are more complicated alternatives to the proposed method. For example, another equation for predicting MRHD was developed during this study

$$\text{MRHD} = \frac{G_r}{3}\sqrt{\frac{K_L}{K_s} - 1} + \frac{D_{ave}}{3}\frac{T_L}{T_s} \tag{13}$$

where K_L = larger of the two frame stiffnesses; K_s = smaller of the two frame stiffnesses; and the restrainer gap value (G_r)

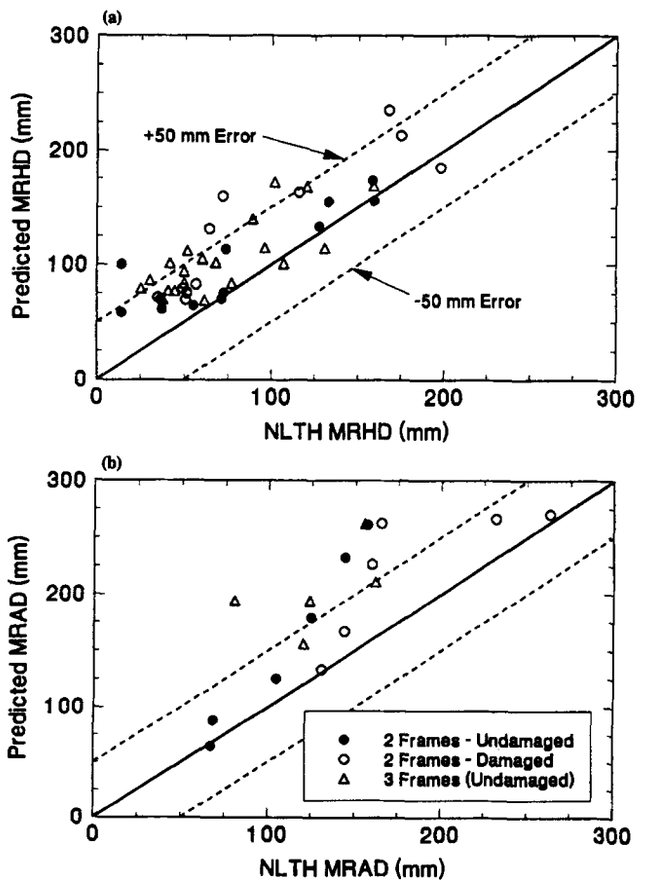

FIG. 14. Effects of Column Damage and Number of Frames on: (a) MRHD; (b) MRAD

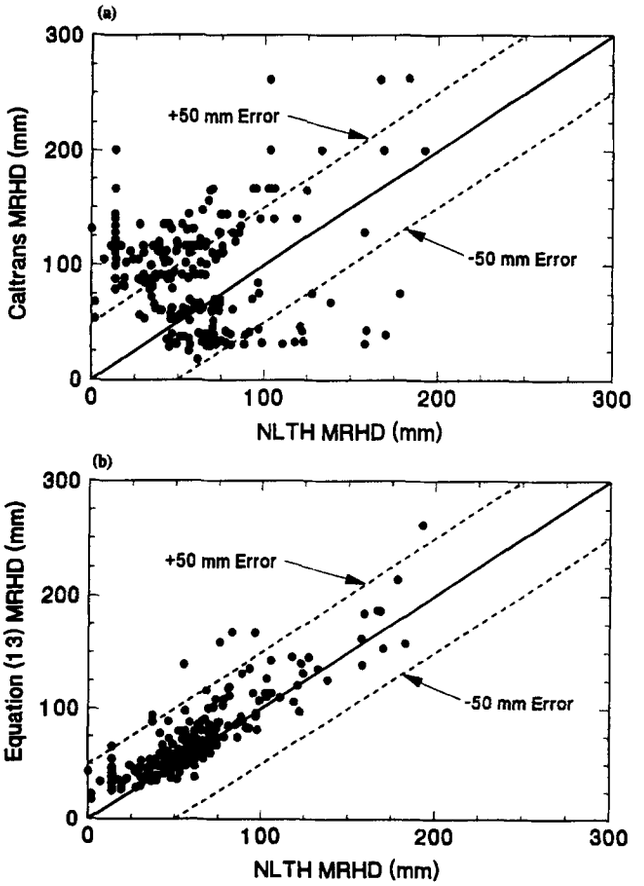

FIG. 15. Comparison of (a) Caltrans Method and (b) Eq. (13) with NLTH

is limited to 100 mm, even when $K_r = 0.0$. As shown in Fig. 15(b), (13) approximates the NLTH analysis results (mean error = 15 mm) better than does (9). Nonetheless, (9) is proposed for design because it is simpler and more rational. For example, the limit on G_r is arbitrary.

IMPLEMENTATION

In the design examples, the proposed methods for predicting MRHD and MRAD were applied without a factor of safety. Effects that were not included in the study, such as differential seismic inputs due to ground-motion incoherency, topography, and variations in soil conditions, could increase the relative displacements. In practice, a designer might wish to increase the computed MRHDs and MRADs to account for these effects.

SUMMARY AND CONCLUSIONS

The seismic behavior of bridges containing in-span hinges equipped with restrainers was studied analytically by subjecting 216 models to earthquake motions. The models simulated the longitudinal motion of straight bridges without skew and neglected soil-structure interaction and ground-motion spatial variation.

The maximum relative displacement at the in-span hinge (MRHD) depended primarily on the frame stiffnesses, the frames' relative periods, and the restrainer stiffness and gap. The maximum relative displacement at the abutment (MRAD) depended primarily on the overall stiffness and mass of the bridge.

Based on the parametric study, a procedure was developed for approximating the MRHD. The method is similar to the Caltrans equivalent static analysis method (*Seismic* 1990), but the proposed method relies on a new equation to estimate the MRHD (9). In comparison with the Caltrans method, the proposed method predicts values of MRHD that are more consistent with the values computed by nonlinear time-history analyses.

The proposed method is an improvement on the AASHTO method (1994) because the restrainer gap, area, and length can be selected rationally, taking into account the frame stiffnesses and effective periods. The proposed method for estimating the MRAD is simple and gives results that are conservative compared with the values obtained from nonlinear time-history analyses.

ACKNOWLEDGMENTS

The research was funded primarily by the Washington State Department of Transportation (WSDOT) and the Federal Highway Administration. Jim Wei served as the WSDOT technical contact. The authors thank Sadaaki Nakamura and Mattheus Schulze for performing case studies of bridges.

APPENDIX. REFERENCES

AASHTO LRFD bridge design specifications; SI Units, First Edition. (1994). Am. Assn. of State Hwy. and Transp. Officials, Washington, D.C.

Lwin, M. M., and Henley, E. H. (1993). *Bridge seismic retrofit program report*, Washington State Dept. of Transp., Olympia, Wash.

Prakash, V., Powell, G. H., and Campbell, S. (1993). "DRAIN-2DX base program description and user guide." *Rep. No. UCB/SEMM-93-17*, Dept. of Civ. Engrg., Univ. of California, Berkeley, Calif.

Roberts, J. E. (1991). "Research based seismic design and retrofit of California bridges." *Proc., 1st Annu. Seismic Res. Workshop*, California Dept. of Transp., Sacramento, Calif.

Saiidi, M., Maragakis, E., and Feng, S. (1992). "An evaluation of the current Caltrans seismic restrainer design method." *Rep. No. CCEER 92-8*, Dept. of Civ. Engrg., Univ. of Nevada, Reno, Nev.

Seismic design references. (1990). California Dept. of Transp., Sacramento, Calif.

Stanton, J. F., and Roeder, C. W. (1982). "Elastomeric bearings design, construction and materials." *Rep. No. 248*, Nat. Cooperative Hwy. Res. Program, Washington, D.C.

Trochalakis, P., Eberhard, M. O., and Stanton, J. F. (1996). "Design of seismic restrainers for in-span hinges." *Rep. No. WA-RD 387.1*, Washington State Dept. of Transp., Olympia, Wash.

Yang, Y.-S. (1994). "Aspects of modeling of reinforced concrete bridge structures for dynamic time history analysis," PhD thesis, Univ. of California, San Diego, Calif.